

Synthesis of immobilized chitosan/humic acid coupling product for removal of Pb(II), Cd(II) and Cr₂O₇²⁻ from aqueous solutions

Frezah J. Muhana^a, Bassam I. El-Eswed^{b,*}, Fawwaz I. Khalili^c

^aAl-Ahliyya Amman University, Amman, Jordan, email: f.muhana@ammanu.edu.jo

^bZarqa College, Al-Balqa Applied University, P.O. Box 313, Zarqa 13110, Jordan, email: bassameswed@bau.edu.jo

^cChemistry Department, The University of Jordan, Amman 11942, Jordan, email: fkhalili@ju.edu.jo

Received 27 February 2017; Accepted 2 August 2017

ABSTRACT

Immobilized coupling product (CP) of chitosan with humic acid was prepared to overcome the solubility limitations in using chitosan and HA as adsorbents for heavy metal ions. Two CPs were prepared; FCP from Fluka humic acid and JCP from Ajloun (Jordan) humic acid. The prepared CPs were found to be insoluble in the pH range from 2 to 12. The CPs were studied by elemental analysis, Ba(OH)₂ titration, potentiometric titration, FTIR, solid ¹³C-NMR, SEM and XRD. The results indicated the formation of covalent amide/ester bonds and electrostatic bonds (~~~NH₃⁺...OOC~~~) between chitosan and humic acid. The uptake of Pb(II) and Cd(II) by CPs was found to increase with increasing pH and ionic strength, while the reverse was observed in the case of Cr₂O₇²⁻ which indicated a unique behavior of CPs compared with free humic acid and chitosan. The adsorption capacities of Pb(II), Cd(II), and Cr(VI) were 33.0, 24.7, and 56.5 mg/g, respectively, in the case of FCP, and 54.9, 20.1, and 54.1 mg/g, respectively, in the case of JCP. The effect of time and temperature on adsorption showed that it is fast, endothermic and entropy driven. The SEM indicated tight surface of CPs due to the strong bonding between chitosan and humic acid. To overcome this problem, CPs were modified by spread over silica gel to produce a high capacity adsorbent (486 mg Pb/g FCP) which has superior removal of low concentrations of Pb < 30 ppm with about 100% efficiency.

Keywords: Adsorption; Cadmium; Chitosan; Dichromate; Humic acid; Lead

1. Introduction

Heavy metal ions are toxic and have adverse effect on human being [1], even at low concentration [2]. Separation of heavy metals from water is an important target for environmental research since they are not biodegradable and thus could accumulate in our environment [3]. Lead is one of the most dangerous elements in soil, air and water. Aquatic environment could be polluted with lead from waste of industrial plants like fertilizers, batteries, pesticides, and solder [4]. While cadmium comes from earth's crust, fossil fuels, smelting, plastic industry, metal plating, electronic industry, and tobacco fume [5]. Mean while chromium exists naturally in volcanic dust, soil, and rocks. The most common oxidation states of chromium are Cr(III) and Cr(VI) [6]. The latter is a strong oxidizing agent that is used

in many industrial processes, such as printing, leather tanning and steel manufacturing. Cr(VI) is the most toxic form of chromium since it is highly soluble and can enter the biological cells causing dermatotoxicity, neurotoxicity, genotoxicity, and carcinogenicity [7,8].

Chitosan (poly(β-1-4)-2-amino-2-deoxy-D-glucopyranose) is a biopolymer produced from *N*-deacetylation of chitin, a major component of crustacean shells, and is readily available from seafood-processing wastes. The high proportion of amino functions in chitosan provide binding properties for many metal ions [9]. Chitosan is an economical, efficient, and safe biosorbent from marine waste [10]. Consequently, many studies have been conducted on using chitosan flakes or hydrogel beads for heavy metal removal from wastewater [9,11].

Since chitosan is normally soluble at pH < 6.5 [12], neutral and basic media are not suitable for studying adsorption because of precipitation of heavy metals and since most

*Corresponding author.

polluted industrial effluents are acidic. Furthermore, flake and powder forms of chitosan are not suitable for use as adsorbents for heavy metal ions due to their low surface areas and nonporosity. This can be avoided by casting chitosan beads with high porosity and large surface area materials followed by crosslinking to make beads stable in acidic medium. Although crosslinking enhances resistance of chitosan to acids, it reduces its adsorption capacity [13]. Several crosslinking agents were proposed for reinforcement of chemical stability of chitosan like glutaraldehyde, ethylene glycol, diglycidyl ether, epichlorohydrin and tripolyphosphate [14]. The adsorption capacity of Pb(II) onto chitosan beads crosslinked with glutaraldehyde was 79.2 mg/g [15] and the adsorption capacity of Cr(VI) on chitosan nanoparticles crosslinked with tripolyphosphate was 68.9 mg/g [14].

Humic acid (HA) is a subclass of humic substances (major component of soil organic matter) and generally displays macromolecular characteristics. HA contains carboxylic and phenolic groups and consequently can carry negative charge in aqueous solutions [9]. HA is soluble in aqueous solution, and precipitate as colloidal material when pH is decreased below 2 [15]. HA can effectively adsorb different heavy metal ions from aqueous solution and thus, it affects the fate of contaminants in soils and sediments [16].

Although the complexation of HA with heavy metal ions was studied extensively, it is very difficult to use HA as a solid adsorbent for heavy metal ions because of its solubility in water at $\text{pH} > 2$ [16]. Several methods have been used to decrease the solubility of HA by heating at 330°C and using supports like calcium alginate gel and activated carbon. These treatments of HA resulted in significant decrease in the adsorption capacity of HA [17]. Zhao and Binjiang prepared HA coated Fe_3O_4 nanoparticles ($\text{Fe}_3\text{O}_4/\text{HA}$) for the removal of heavy metals from water with adsorption capacities from 46.3 to 97.7 mg/g. The $\text{Fe}_3\text{O}_4/\text{HA}$ composite was effective in removing more than 95% of Hg(II), Pb(II), Cu(II) and Cd(II) from natural and tap water. The $\text{Fe}_3\text{O}_4/\text{HA}$ is stable in tap water, natural waters, acidic and basic solutions [18].

Chitosan and HA were reported to interact strongly with each other. The adsorption capacity of humic acid on chitosan was reported to be 28.88 mg/g at pH 3.07 and decrease with the increase of pH [11]. The adsorption of HA on chitosan (coated on polyethyleneterephthalate granules) was found to be pH dependent; strong at $\text{pH} \leq 6.5$ and weak at basic conditions. X-ray photoelectron spectroscopy (XPS) indicated the formation of organic complex between the protonated amino groups of the chitosan and carboxylates of HA. The amino groups in the chitosan ($\text{pK}_a = 6.3\text{--}6.6$) were protonated in the acidic medium and subsequently interacted with the carboxylic groups of HA to form the organic complexes $\text{---NH}_3^+ \cdots \text{---OOC---}$ [9, 11]. Zeta potential measurements indicated that at $\text{pH} > 3$, the carboxylic groups of HA are dissociated into carboxylates and the amine groups of chitosan are protonated, which support the same mechanism of interaction [19]. Wan Ngah and Hanafiah suggested the same mechanism depending on their results of adsorption of HA on chitosan beads (cross-linked with epichlorohydrin). The adsorption capacity was found to be 44.84 mg HA/g chitosan [20].

Santosa et al. [21] prepared a hybrid of HA and chitin by mixing gelatinous chitin (dissolved in HCl solution) and HA (dissolved in NaOH solution) in 20:1 mass ratio.

The immobilization of HA on chitin was assumed to occur through condensation reaction between the protonated N-acetyl group of chitin and carboxylate of HA. The chitin-HA coupling product showed slightly higher metal-ion adsorption capacity (5.9 mg/g) towards Ni(II) than chitin alone (4.4 mg/g). The interesting finding of this study was that the Langmuir affinity constant K_L of chitin-HA (5892 L/mol) was much higher than that of chitin (11.86 L/mol). The extremely high K_L value is an indication that chitin-HA product is efficient in removal of Ni(II) even at very low concentrations of Ni(II) [21]. The adsorption capacity of Cd(II) on hybrid of chitosan-HA (using glutaraldehyde cross-linker) was extremely high 334 mg/g [22]. However, the problem was that the adsorption experiments in these studies were carried out using high metal concentration at pH 7 which causes precipitation of metal ions.

Repo et al. [23] investigated adsorption of Co(II) and Ni(II) on chitosan modified with ethylenediaminetetraacetic acid (EDTA) or diethylenetriaminepentaacetic acid (DTPA). The produced EDTA-chitosan and DTPA-chitosan products were very stable in 2 M HNO_3 solution and thus could be regenerated after being used as adsorbents for heavy metals. The maximum adsorption capacity of Co(II) and Ni(II) were 63.0 and 71.0 mg/g, respectively, in the case of EDTA-chitosan and 49.1 and 53.1 mg/g, respectively, in the case of DTPA-chitosan. This chemical modification of chitosan improved remarkably its adsorption capacity (2.5 mg/g in the case of adsorption of Co(II) by unmodified chitosan). The effect of pH on adsorption was significant because as the pH increased from 1 to 2, the % uptake of Co(II) by EDTA-chitosan increased from 20 to 90% [23]. Similar modification was reported by reacting chitosan with ethylene glycol-bis(2-aminoethylether)-N,N,N,N'-tetraacetic acid (EGTA). The adsorption capacity of Pb(II) and Cd(II) by EGTA-chitosan were 103.6 and 84.3 mg/g, respectively. It was shown that the adsorption capacity is fast and within 5 min, 60–70% of the maximum uptake of Pb(II) and Cd(II) were removed by EGTA-chitosan. The adsorption mechanism was assumed to be coordination of Pb(II) and Cd(II) to carboxyl oxygens and aminenitrogens to form stable chelates [24].

In the same line of research, Zhao et al. prepared magnetic chitosan by reacting chitosan with Fe_3O_4 nanoparticles using glutaraldehyde, EDTA and DTPA as crosslinkers. The magnetic EDTA-chitosan and DTPA-chitosan were found to have remarkably higher metal removal than glutaraldehyde crosslinked magnetic chitosan. The maximum adsorption capacity of Cd(II), Co(II), Pb(II) and Ni(II) by magnetic EDTA-chitosan were huge 168.6, 73.1, 213.4 and 81.0 mg/g, respectively. On the other hand, the removal of oxyanion species $\text{Cr}_2\text{O}_7^{2-}$, H_2AsO_3^- and H_2AsO_4^- was relatively low [25].

Both HA and chitosan are potential adsorbents for heavy metal ions. The solubility of HA at $\text{pH} > 2$ and the solubility of chitosan at $\text{pH} < 6.5$ imposed strong limitations on their industrial applications as adsorbents. The aim of the present work is to prepare a coupling product from chitosan and humic acid (HA) that is insoluble in the adsorption pH working range of 2–6. The stability of the coupling product under different pH values will be studied and the nature of interaction between chitosan and HA will be investigated using elemental analysis, potentiometric titration, FTIR, ^{13}C -NMR, SEM and XRD analysis. The coupling product will be evaluated for adsorption of metal cations

Pb(II), and Cd(II) and metal oxyanions ($\text{Cr}_2\text{O}_7^{2-}$) at different conditions (pH, ionic strength, metal concentration, contact time and temperature).

In order to evaluate the effect of the origin of HA on the physicochemical properties and adsorption behavior of the coupling product, two sources of HA were used, one from Fluka (FHA) and the other was extracted from Ajloun-Jordan (JHA).

2. Experimental

2.1. Materials

All chemicals were purchased from commercial sources as either analytical reagent grade or chemically pure grade and were used as received. $\text{Pb}(\text{NO}_3)_2$ was from AVONCHEM, $\text{Cd}(\text{NO}_3)_2 \cdot 4\text{H}_2\text{O}$ from BDH, NaOH from LOBA, NaNO_3 from Riedel-dehaen, $\text{K}_2\text{Cr}_2\text{O}_7$ from UNI-CHEM, KMnO_4 from Fluka, HCl 37% from TEDIA, KCl and AgNO_3 from Puriss, and ninhydrin from BIO BASIC INC. Silica gel (60–200 micron) was from SDS. Chitosan (degree of deacetylation (DD) ≥ 75) was from Sigma. Two types of humic acid were used; one from Fluka (FHA) and the other (JHA) was extracted from Ajloun soil (North of Jordan) using the method of the International Humic Substance Society (IHSS, <http://www.humicsubstances.org/soilhafa.html>).

2.2. Preparation of coupling products of chitosan with humic acid

A sample of 2.50 g of chitosan was dissolved in 150 mL of 0.10 M HCl solution and a separate sample of 2.50 g humic acid (FHA or JHA) was dissolved in 150 mL of 0.10 M NaOH solution. The two solutions were mixed with stirring and aged for 6 h at 45°C and then for 24 h at room temperature. The product was collected by filtration and the resulting brown coupling product was dried at 70°C for 24 h and sieved through mesh size (250 μm). The coupling products prepared from Fluka humic acid and Ajloun-Jordan humic acid were given the abbreviations FCP and JCP, respectively.

2.3. Characterization of coupling products of chitosan with humic acid

2.3.1. Solubility and stability of coupling products

A 0.10 g sample of FCP or JCP was shaken (GFL-1083 shaker) with 50.0 mL deionized water adjusted to pH values of 2.0, 4.0, 6.0, 8.0, 10.0, and 12.0 (WTW in Lab 720 pH meter). The stability of the coupling product was tested by measuring the absorbance value (Varian Cary 100 UV-Visible spectrophotometer) of these solutions after filtration. The absorbance of HA was measured at 254 nm [26] and the absorbance of chitosan was measured at 570 nm for the chitosan-ninhydrin complex [27].

2.3.2. Total acidity

In a 100-mL polyethylene vessel, 0.0500 g of FHA, JHA, FCP and JCP samples were shaken with an excess of 0.10 M $\text{Ba}(\text{OH})_2$ (50.0 mL) solution under nitrogen for 24 h. The

suspensions were filtered, washed and the filtrates were titrated with 0.10 M HCl solution to $\text{pH} = 8.4$. A blank solution of 50.0 mL of 0.10 M $\text{Ba}(\text{OH})_2$ was subjected to the same procedure [28].

2.3.3. Potentiometric titration

The titration curves were obtained by addition of small increments of 0.050 M NaOH to 50.0 mL of deionized water containing 0.1000 g of sample under nitrogen [29]. The pH was measured after each addition under continuous flow of nitrogen gas.

Elemental analysis was done using Euro Vector 3000 Elemental Analyzer. FTIR spectra were recorded using Thermo Nicolet NEXUS 70 spectrophotometer. XRD patterns were obtained by Shimadzu XRD 6000 equipped with $\text{CuK}\alpha$ radiation source using Ni as filter and operated at 30 kV/30 mA. The FEI inspect F50 scanning electron microscopy was used to record SEM graphs of the samples after coating with platinum. Solid ^{13}C -NMR spectra were obtained using Bruker DPX-500 spectrometer.

2.4. Adsorption experiments

2.4.1. Effect of pH

A 25.0 mL of stock solution (200 ppm) of metal ion was added into 100-mL volumetric flask and was diluted with deionized water until reached about 90 mL. The solution was transferred into a beaker and the pH was adjusted to 6.0 using drops of 0.050 M HCl or 0.050 M NaOH . Then the solution was returned into the volumetric flask and deionized water was added to the mark. The process was repeated and the pH was adjusted to 2.0, 3.0, 4.0 and 5.0. Each 100.0 mL solution was divided into two 50.0 mL portions in closed plastic containers and 0.0500 g of coupling products (FCP or JCP) was added to one portion and the second portion was kept as a reference standard. The ten plastic containers were placed in the shaker for 24 h, and then the solutions were filtered and the concentrations of metal ions were determined using atomic absorption spectrometer (Varian Spectra AA-250 pulse).

The equilibrium amount of metal ions adsorbed (q_e , mg/g) by the coupling product was obtained using Eq. (1):

$$q_e = \frac{(C_i - C_e)V}{m} \quad (1)$$

where C_i is the initial metal ion concentration (ppm), C_e is the remaining concentration of the metal ion in solution after adsorption (ppm), V is the volume of solution (L) and m is the mass of adsorbent (g). The percentage of metal uptake was calculated using Eq. (2) [30]:

$$\% \text{Metal uptake} = \frac{(C_i - C_e)}{C_i} \times 100\% \quad (2)$$

2.4.2. Effect of ionic strength

The effect of pH experiments were repeated using 0.50 M NaNO_3 solution instead of deionized water in preparation of stock, standard and sample solutions.

2.4.3. Adsorption isotherms

The adsorption isotherms were obtained by agitating 0.0500 g of coupling product with 50.0 mL of varying concentrations of metal ions from 10 to 200 ppm at 25°C. The pH of the solutions of Pb(II) and Cd(II), was adjusted to 5.5, while the pH of the solution of Cr(VI) was adjusted to 2.0. The solutions were shaken for 24 h. The suspensions were filtered, and the filtrates were analyzed for metal ions concentration.

2.4.4. Kinetic study

A 0.0500 g of coupling product was placed in a flask containing 50.0 mL of 100 ppm metal ion solution. The pH of the solution was fixed at 5.5 in the case of Pb(II) and Cd(II) from 2.0 in the case of Cr(VI). The flasks were shaken for different times range 5 min to 32 h, then the solutions were filtered and the metal concentrations were determined.

2.4.5. Effect of temperature

A 0.0500 g of coupling product samples were placed in flasks containing 50.0 mL of 100 ppm metal solution. The pH of the solution was fixed at 5.5 in the case of Pb(II) and Cd(II) and at 2.0 in the case of Cr(VI). The flasks were shaken at 25, 35, 45 and 55°C. After 24 h, the suspensions were filtered and the metal concentrations in the filtrates were determined.

2.4.6. Desorption experiments

Desorption of metal-loaded coupling product was conducted by mixing 0.1 g of the loaded coupling product with 0.20 M solutions of NaCl, NaNO₃, Na₂SO₄, HCl, HNO₃ and H₂SO₄ for 24 h. The % desorption was calculated by dividing the amount of metal ion in solution by the concentration of metal ion loaded.

3. Results and discussion

3.1. Characterization of coupling products (FCP and JCP)

3.1.1. Solubility of FCP and JCP

FCP and JCP were insoluble in water and in most known organic solvents like acetone, chloroform, dichloromethane, DMF, DMSO, benzene, pyridine and acetonitrile. Both FCP and JCP were shaken in deionized water adjusted to pH values of 2, 4, 6, 8, 10 and 12. They were found visually to be completely insoluble in this pH range and the stability of the coupling products was further confirmed by measuring the absorbance (Table 1) of these solutions. The absorbance of leached HA was measured at 254 nm [26] and the absorbance of leached chitosan was measured at 570 nm after complexation of ninhydrin [27]. The coupling products were stable and did not decomposed as revealed by the small measured values of absorbance. This indicted the unique property of CP that is different from free chitosan and free HA which are soluble at pH < 6.5 and pH > 2, respectively [12,31]. Thus, the coupling products FCP and JCP could be used as adsorbents for heavy metal ions in the pH range from 2 to 6.

Table 1

Absorbance values of HA and chitosan after leaching of 0.05 g FCP with 50 mL leaching solutions at different pH values

pH of leaching solution	Absorbance at 254 nm for HA	Absorbance at 570 nm for chitosan-ninhydrin complex
2	0.0377	0.000175
4	0.02205	0.00355
6	0.01865	0.006075
8	0.01965	0.006275
10	0.02715	0.010375
12	0.073625	0.0081

3.1.2. Total acidity

The total acidity of FCP, FHA, JCP and JHA was determined by titration with Ba(OH)₂ and found to be 6.30, 11.34, 15.12 and 31.50 mmol/g, respectively. FCP and JCP have less acidic groups than their precursors FHA and JHA. This reduction of acidic groups of HA upon coupling with chitosan is due to the fact that these groups were utilized in binding through the physical/chemical reaction of carboxylic or phenolic groups of HA with the amine or hydroxyl groups of chitosan.

3.1.3 pH-titration curves

The pH titration curves of FCP, FHA and water (as a reference) with NaOH are given in Fig. 1. The pH titration

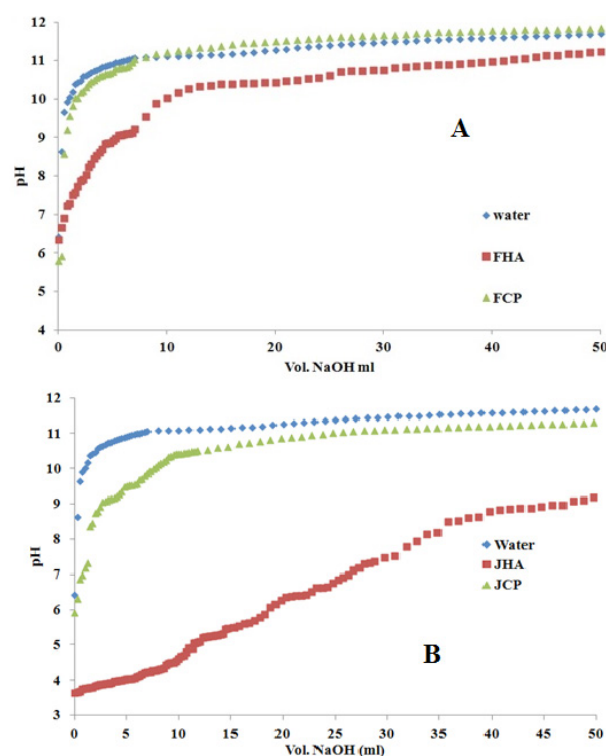


Fig. 1. pH titration curves of A: FCP, FHA, H₂O and. B: JCP, JHA, H₂O.

curve of FHA started from a pH value 6.36 which was close to the pH of water (6.43). However, addition of small amounts of 0.01 M NaOH, raises the pH of water above 10 whereas the solution containing FHA resist increase in pH. The difference between the titration curve of water and that of FHA indicates clearly that FHA contains plenty of acidic sites that can react with NaOH added during the course of titration. The number of these acidic sites was reduced in the coupling product FCP as indicated by the closeness of the curves of FCP and water. Similar behavior was observed in the case of JCP and JHA (Fig. 1).

3.1.4. Elemental analysis

Elemental analyses of chitosan, FHA, JHA, FCP and JCP are given in Table 2. The HA loading on chitosan (% HA) was calculated for FCP and JCP using Eq. (3) which was reported by Zhao et al. for calculation of the loading of ethylene glycol-bis(2-aminoethylether)-N,N,N',N'-tetraacetic acid (EGTA) in the coupling product with chitosan [24].

$$W_{CP} = W_{HA} \times \%HA + W_{chitosan} (1 - \%HA) \quad (3)$$

where W_{HA} , $W_{chitosan}$ and W_{CP} are the nitrogen content of HA, chitosan and coupling product (FCP and JCP), respectively. The percentage of HA in FCP and JCP were calculated to be 47.8% and 56.5%, respectively. These values were close to the percentage of EGTA in EGTA-chitosan found by Zhao et al., which was 50.8% [24].

3.1.5. FTIR study

The FTIR absorption bands of FCP, FHA, JCP, JHA and chitosan are given in Table 3. Analysis of the FTIR data (Table 3) indicated formation of the amide group in the coupling products FCP and JCP which were similar to those found in proteins FTIR [32]. The amide I band of FCP and JCP was observed at 1645 cm^{-1} and 1633 cm^{-1} , respectively and amide II was observed at 1566 and 1576 cm^{-1} , respectively. The amide III was detected at 1384 and 1378 cm^{-1} in the spectra of FCP and JCP, respectively. The C-N stretching band was observed as a strong band at 1473 and 1471 cm^{-1} in the spectra of FCP and JCP, respectively. The N-H out of plane band was detected at 721 cm^{-1} . The C-N stretching and the N-H out of plane bands were well resolved from other bands and appear only in the spectra of the coupling products FCP and JCP. Another interesting band was found at 1725 and 1722 cm^{-1} in the spectra of FCP and JCP, respectively, and

absent in the spectra of starting materials chitosan, FHA and JHA (Figs. 2 and 3). This band is far from the amide range, but close to the ester range [33]. Similar band at 1706 cm^{-1} was observed in the FTIR spectrum of chitosan cross-linked with glutaraldehyde [34]. The main contradiction to the formation of amide or ester bond assumption was the disappearance of this band upon complexation of FCP with Pb(II) (Fig. 2).

Another possible mechanism is the formation of Chitosan $-\text{NH}_3^+ \dots -\text{OOC}-\text{HA}$ physical adduct in the coupling products which could be confirmed by three regions in the spectra:

1. The coupling product has many common features with those reported for zwitter ionic structure of glycine [35]. The most interesting evidence that supports this hypothesis was the effect of coupling reaction on the asymmetric and symmetric stretching vibrations of C-H observed at 2920 and 2850 cm^{-1} in HA and chitosan. Noticeable amplification of the intensity of these bands was observed in the FTIR spectra of FCP (Fig. 3) and JCP. Zwitter ionic glycine showed strong absorption of NH_3 stretching in this region and so this amplification may be due to $-\text{NH}_3^+$ stretching.
2. The bands observed at 1725 and 1722 cm^{-1} in the FTIR spectra of FCP (Fig. 3) and JCP could be assigned to C = O stretching because a similar band at 1745 cm^{-1} in the FTIR of glycine [35].
3. The bands observed at 1473 and 1471 cm^{-1} in the FTIR spectra of FCP and JCP were assigned to intradimeric C-O (H) stretching which is close to that observed in the FTIR spectrum of glycine at 1437 cm^{-1} [35].

Interestingly these three bands disappeared by complexation of the coupling product with Pb(II) (Fig. 2). This indicates that metal ions interrupt the coupling product by chelation between the amino group of chitosan and humic acid carboxylate as shown in Eq. (4):



3.1.6. SEM and XRD

The SEM graphs of FCP and JCP (Fig. 4) indicated a compact tight surface of these materials due to the formation of chemical/physical bonds between the highly

Table 2
Elemental analysis of chitosan, FHA, JHA, FCP and JCP

Polymer	% C	% N	% H	% O*	% ash	% HA in coupling product
Chitosan	40.409	7.468	7.362	44.761	0	
FHA	46.083	1.297	4.472	28.148	20	
JHA	30.444	1.922	3.197	34.437	30	
FCP	42.551	4.518	6.305	36.626	10	47.8%
JCP	35.835	4.335	5.241	39.589	15	56.5%

*%O = 100 - (% C + % N + % H + % ash)

Table 3
FTIR absorption bands of chitosan, FHA, JHA, FCP and JCP*

Assignment assuming covalent coupling	Assignment assuming physical coupling	Chitosan	FHA	JHA	FCP	JCP
H-bonded O-H and NH stretching	H-bonded O-H stretching	3200–3600 (br)	3200–3600 (br)	3200–3600 (br)	3200–3600 (br)	3200–3600 (br)
Aliphatic C-H stretching	Aliphatic C-H and N-H stretching	2922(w) 2850(w)	2920(w) 2843(w)	2920(w) 2850(w)	2920(s) 2850(s)	2932(s) 2833(s)
C = O stretching of ester groups	C = O stretching of carboxylic dimer	–	–	–	1725(s)	1722(s)
C = O stretching of quinones, and amide band (I)	Asymmetric NH ₃ bending, C = O stretching of quinones, and amide band (I)	1643(s)	1632(s)	1633(s)	1645(s)	1633(s)
C = O stretching of quinones, and amide band (II)	C = O stretching of quinones, and amide band (II)	1557(sh)	1570(sh)	1560(sh)	1566(sh)	1576(sh)
Amide C-N stretching	Symmetric NH ₃ bending, C-O(H) stretching of carboxylic dimer	–	–	–	1473(s)	1471(s)
O-H deformation, symmetric stretching of COO ⁻ , and amide band (III)	O-H deformation, symmetric stretching of COO ⁻ , and amide band (III)	1384(s)	1384(m)	1384(m)	1384(s)	1378(s)
C-O stretching of phenolic groups	C-O stretching of phenolic groups	–	–	–	1273(s)	1278(s)
C-O stretching of various aliphatic groups	C-O stretching of various aliphatic groups.	1157(s) 1080(s)	1097(sh) 1038(s)	1114 (sh) 1036(s)	1118(s) 1070(s)	1163(sh) 1121(s) 1068(s) 1025(s)
N-H out of plane bending	N-H out of plane bending	–	–	–	721(s)	721(s)

*Broad (br), strong (s), medium (m), weak (w) and shoulder (sh). Assignment of HA bands were according to Refs. [51,52]. Assignments of chitosan bands were according to Ref. [14,34]. Assignments of coupling products bands were according to Ref. [32,35].

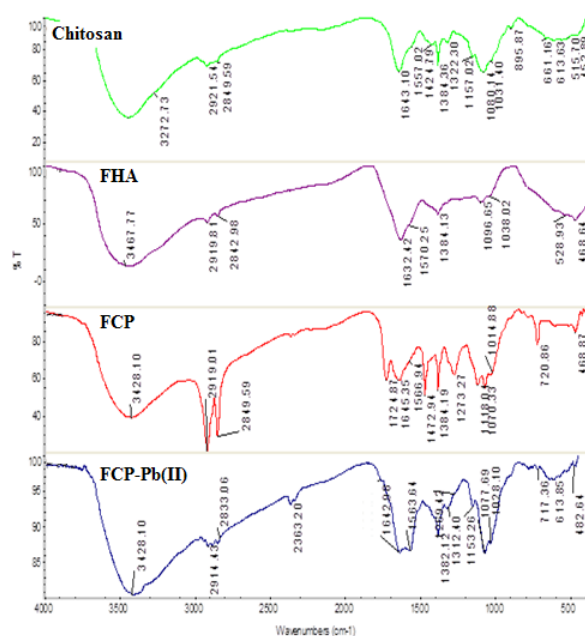


Fig. 2. FTIR spectra for chitosan, FHA, FCP and FCP-Pb(II) complex.

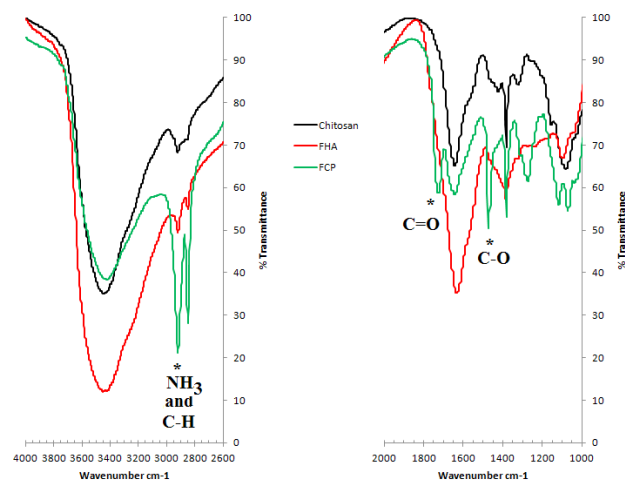


Fig. 3. FTIR spectra for FCP, FHA and chitosan.

functionalized HA and chitosan. The XRD patterns (Fig. 5) showed some crystallinity in the coupling products similar to that found in HA and chitosan.

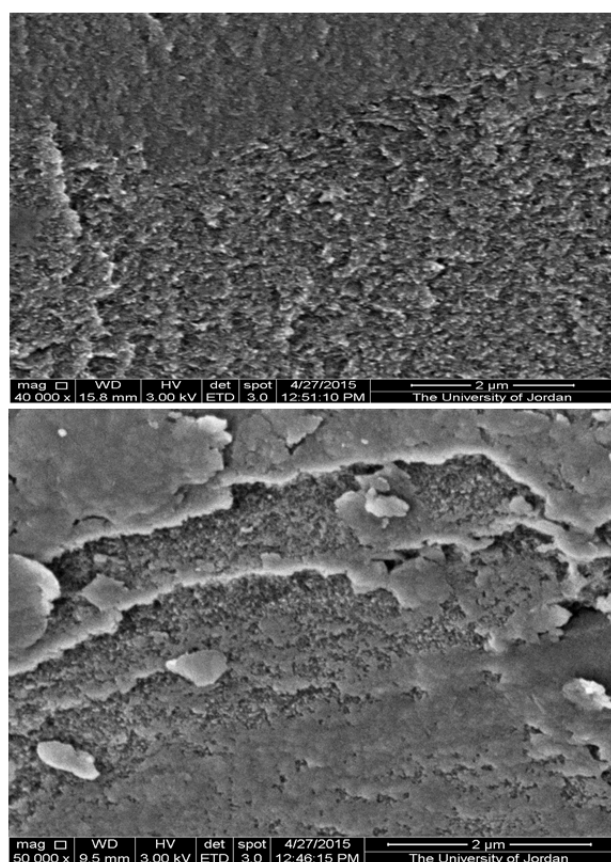


Fig. 4. SEM micrograph for FCP (top) and JCP (bottom) at magnifications 40000x.

3.1.7. Solid ^{13}C -NMR

The Solid ^{13}C -NMR spectra of FCP, FHA, JCP, JHA, and chitosan are given in Fig. 6. Only the aliphatic part of HA was detected in the spectra at 32 ppm while the carbonyl and aromatic carbons were hardly detected. Since no fundamental changes occurred upon coupling, the spectra supported the idea that physical rather than chemical reaction occurred between chitosan and HA.

3.2. Adsorption studies

3.2.1. Effect of pH on metal-ion uptake

The pH dependence of metal ions uptake (Fig. 7) was investigated in the pH range from 2.0 to 6.0 under continuous shaking of metal ions solutions with solid FCP or JCP for a fixed contact time of 24 h at 25°C and ionic strength $I = 0.0$ and 0.5 M. High pH values above 6.0 were avoided to prevent precipitation of the metal ions as hydroxides which interfere with adsorption.

The % uptake of Pb(II) by FCP and JCP was found to increase dramatically from less than 5% to more than 75% with increase of pH of solutions from 2.0 to 6.0. On the other hand, the % uptake of Cd(II) on FCP and JCP were found to increase from less than 6% to about 30% with increase of pH of solutions from 2.0 to 6. The

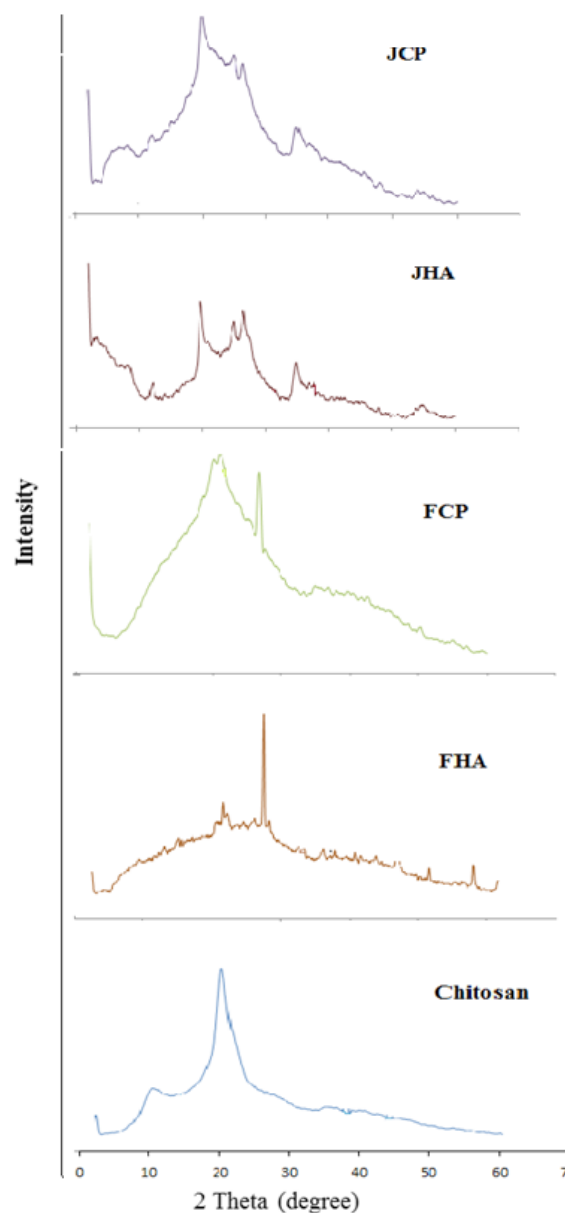


Fig. 5. XRD pattern of chitosan, FHA, FCP, JHA and JCP.

pH-dependent functional groups expected to be available in FCP and JCP are the carboxylic, phenolic groups (from HA), and amine groups (from chitosan). The carboxylic groups of HA have $\text{pK}_a = 2.9$ [36], so they are expected to be active sites (deprotonated) in the pH range from 2 to 6. On the other hand, phenolic groups with $\text{pK}_a = 8.0$ [36] and amine groups with $\text{pK}_a = 6.3\text{--}7.2$ [37] are not expected to participate in adsorption because they are protonated the range of pH from 2 to 6. At pH 2, there will be a great competition between the H^+ present in solution and cationic Pb(II) and Cd(II) for adsorption on the carboxylate sites of the coupling product. Thus, the increase of pH will decrease competition of H^+ with Pb(II) and Cd(II) on interaction with the carboxylate groups.

The % uptake of $\text{Cr}_2\text{O}_7^{2-}$ by FCP and JCP were found to increase from less than 6% to more than 50% with decrease

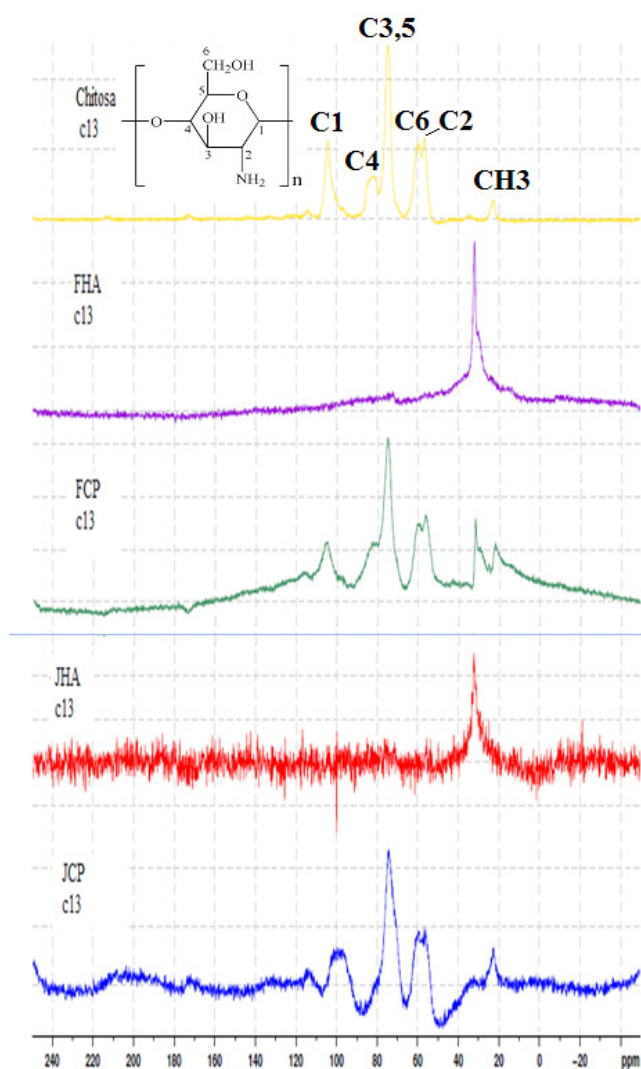


Fig. 6. Solid ^{13}C -NMR spectra of chitosan, FHA, FCP, JHA, JCP.

of the pH of the solutions from 6.0 to 2.0 (Fig. 7). Decreasing the pH causes protonation of amine groups and makes interaction with anionic $\text{Cr}_2\text{O}_7^{2-}$ more favored. Thus, in the coupling products, carboxylates groups contributed by HA are the most probable sites for adsorption of Pb(II) and Cd(II) while ammonium form of amine groups contributed by chitosan are the active sites for adsorption of anionic $\text{Cr}_2\text{O}_7^{2-}$.

Shaker et al. [38] reported an increase of adsorption of $\text{Cr}_2\text{O}_7^{2-}$ on HA with increase of pH. Dima et al. [14] reported an increase of $\text{Cr}_2\text{O}_7^{2-}$ adsorption on chitosan with increase of pH. In the present work, the unique behavior observed for increasing $\text{Cr}_2\text{O}_7^{2-}$ adsorption on FCP and JCP with decreasing pH indicated that the coupling products are different from free HA and free chitosan. However, Dima et al. [14] found that the adsorption of $\text{Cr}_2\text{O}_7^{2-}$ on chitosan cross-linked with tripolyphosphate increases with decreasing pH, which is a similar behavior to what has been observed in the present work.

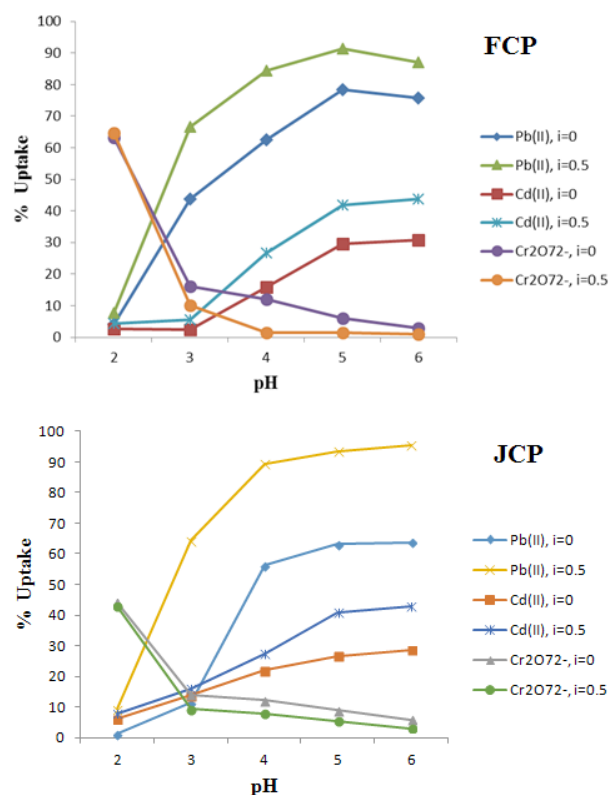
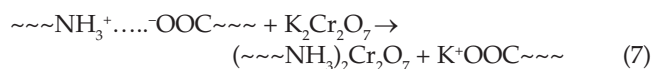
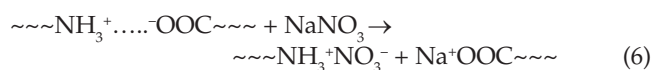
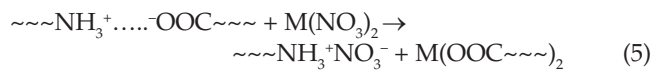


Fig. 7. Effect of pH on Pb(II), Cd(II), $\text{Cr}_2\text{O}_7^{2-}$ uptake by FCP and JCP at ionic strength = 0 and 0.5.

The adsorption of the anions permanganate MnO_4^- and nitrate NO_3^- on FCP and JCP was studied, but no detectable amounts of these anions were adsorbed in the pH range from 2.0 to 6.0.

3.2.2. Effect of ionic strength on metal-ion uptake

Kinniburgh et al. showed that the negative charge on HA decreases as the ionic strength increases. Furthermore, increasing ionic strength increases the competition between the cation of the added electrolyte (Na^+ for examples) and the metal ion adsorbed [39]. Also it was reported that aggregation of HA coils in highly ionic strength media, makes adsorption sites less accessible to metal ions [40]. Thus, increasing ionic strength of solutions should reduce adsorption of Pb(II) and Cd(II) on FCP and JCP if they have similar character to HA and chitosan. Actually, the reverse was observed in the present work. Fig. 7 shows that the % uptake of Pb(II) and Cd(II) increases with increasing ionic strength from $I = 0.0$ to 0.5 M NaNO_3 . This is a clear evidence for the unique behavior of FCP and JCP when compared with HA and chitosan. The positive effect of Na^+ on adsorption of Pb(II) and Cd(II) may be due to ability of Na^+ to disrupt the $\sim\sim\sim\text{NH}_3^+\dots\text{OOC}\sim\sim\sim$ aggregate and thus facilitates carboxylate sites to chelate Pb(II) and Cd(II). There is no competition between M^{2+} [Eq. (5)] and Na^+ [Eq. (6)] because the interaction of M^{2+} with carboxylate is not electrostatic, rather it is specific chemical chelation.



However, in the case of adsorption of $\text{Cr}_2\text{O}_7^{2-}$ onto FCP and JCP (Fig. 7), which is typical electrostatic interaction, increasing ionic strength caused a decrease in the % uptake. This can be explained by the fact that increasing ionic strength using NaNO_3 will increase the competition between NO_3^- [Eq. (6)] and $\text{Cr}_2\text{O}_7^{2-}$ [Eq. (7)] for electrostatic interaction with the positively charged protonated amine groups of FCP and JCP.

3.2.3. Adsorption isotherms

The adsorption isotherms of Pb(II) and Cd(II) were carried out at ionic strength = 0.0 and pH = 5.5 for 24 h. On the other hand, the adsorption isotherms of $\text{Cr}_2\text{O}_7^{2-}$ were performed at pH 2.0 because this pH gives the highest uptake for $\text{Cr}_2\text{O}_7^{2-}$ (Section 3.2.1). The plots of adsorption isotherms are given in Fig. 8. The Langmuir model [Eq. (8)] was widely used to fit adsorption isotherms [41]:

$$q_e = \frac{q_m K_L C_e}{(1 + K_L C_e)} \quad (8)$$

where q_e is the equilibrium amount of adsorbate per unit mass of adsorbent (mg/g), C_e is the equilibrium concentration of adsorbate (mg/L), q_m is the adsorption capacity of the monolayer (mg/g), and K_L is the Langmuir constant related to the energy and affinity of binding sites of adsorption (L/mg) [42]. A linearized Langmuir form [Eq. (9)] can be obtained by taking the inverse of both sides of Eq. (8) and multiplying by C_e [43]:

$$\frac{C_e}{q_e} = \frac{1}{(q_m K_L)} + \left(\frac{1}{q_m}\right) C_e \quad (9)$$

Linear Langmuir plots of C_e/q_e versus C_e gave straight lines (Fig. 8) so that the slopes can be used to determine the adsorption capacities q_m and the intercepts can be used to calculate the affinity constants K_L (Table 4). The interesting finding was that FCP and JCP has a unique affinity to adsorb both metal cations Pb(II) and Cd(II) and anions ($\text{Cr}_2\text{O}_7^{2-}$). This is due to the presence of carboxylate that is accessible for metal cations and also ammonium groups that can attract metal anions.

The Pb(II) had higher q_m values than Cd(II) which can be explained depending on Hard and Soft Acids and Bases principle (HSAB). HSAB predicts that Pb(II) is a softer cation than Cd(II) that is capable of forming stronger surface complexes with soft Lewis bases such as carboxylate [44].

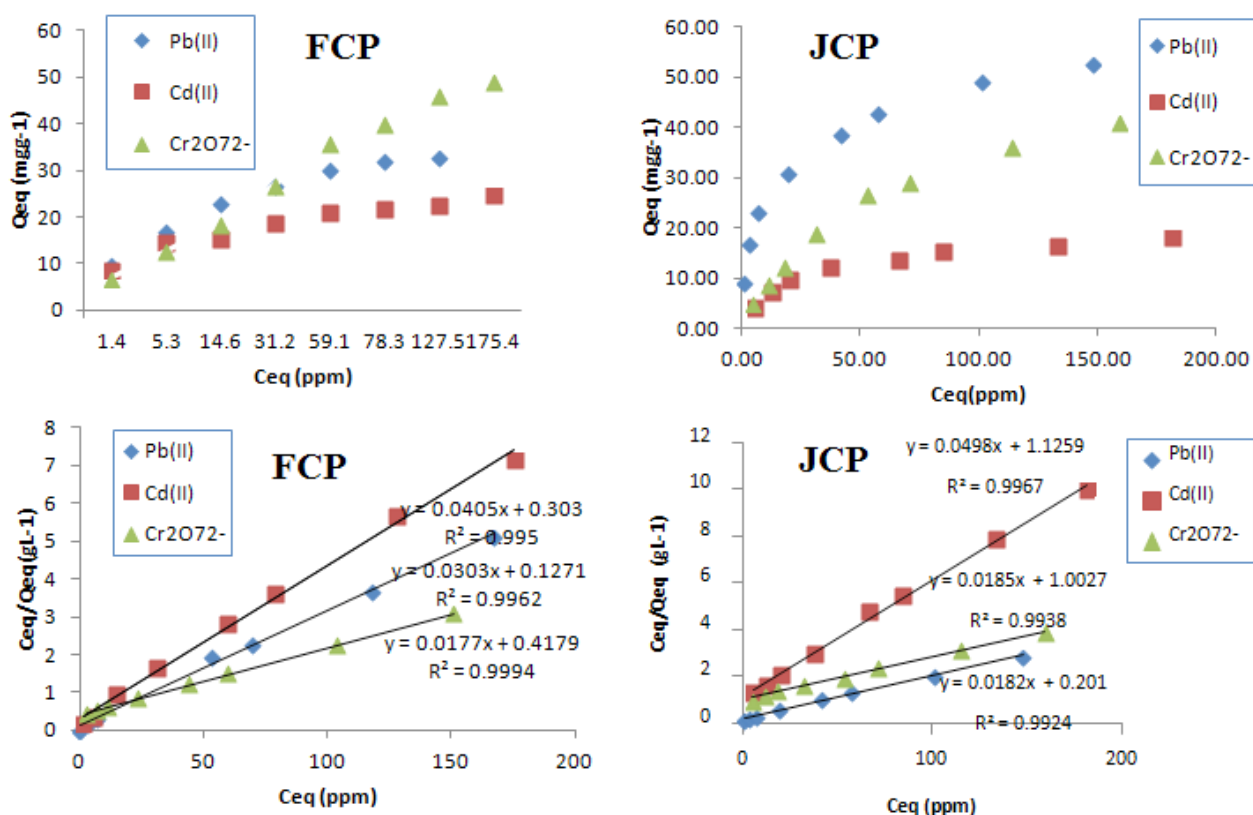


Fig. 8. Adsorption isotherms of Pb(II), Cd(II) and $\text{Cr}_2\text{O}_7^{2-}$ by FCP and JCP at 25°C.

The adsorption capacity of free chitosan toward Pb(II) was reported to be 0.73 mmol/g at pH 5 [45], and the adsorption capacity of chitosan toward Cr(VI) was reported to be 4.81 mmol/g [14]. Attempts to blend chitosan in order to reduce its solubility resulted in reduction of q_m of Pb(II) to 0.36 mmol/g in the case of chitosan cross-linked using glutaraldehyde [13], 0.16 mmol/g for Cd(II) in the case of chitosan nanoparticles prepared by emulsion crosslinking with glutaraldehyde [34], and 1.33 mmol/g for Cr(VI) in the case of chitosan cross-linked with tripolyphosphate [14]. These reported values for cross-linked chitosan are comparable or smaller than those found in the present work for FCP and JCP (0.2–1.0 mmol/g, Table 4). Thus, one can arrive to the conclusion that cross-linking or coupling of chitosan, although results in reduction of solubility of chitosan, results in reduction of adsorption capacity due to reduction in surface functional groups.

The adsorption capacity of Cu(II) on solid HA at pH 2.0 was reported to be 0.16 mmol/g [16]. Also, if HA was subjected to thermal treatment (to decrease HA solubility in water), the q_m value of adsorption of Pb(II) was reported to be 0.19 mmol/g [17]. The values of q_m obtained in the present work for adsorption of Pb(II) on FCP and JCP (0.2–1.0 mmol/g), were higher than those of thermally treated HA. Furthermore, coupling of HA with chitosan has the advantage of reducing the toxicity resulted from dissolving of HA during adsorption of heavy metal ions and the bad side effects on health mentioned in the introduction.

However, we believe that the huge functionality of HA and chitosan are enough to satisfy coupling reaction with plenty of functional groups remaining after coupling. Actually, the reason beyond reduction of adsorption capacity of FCP and JCP may be due to the strong physical/chemical bonding between the HA and chitosan moieties in the coupling products. Thus, it was worth to test adsorption capacity of FCP prepared in the presence of large surface area silica gel (60–200 microns). The fabricated FCP/silica product was found to have high adsorption capacity towards Pb(II) (Fig. 9) which reached 44.25 mg Pb(II)/g FCP-Silica which is equivalent to 486 mg Pb(II)/g FCP assuming that silica gel has low adsorption capacity toward of Pb(II). Tran et al. reported an adsorption capacity q_m of 1.86 mg/g for

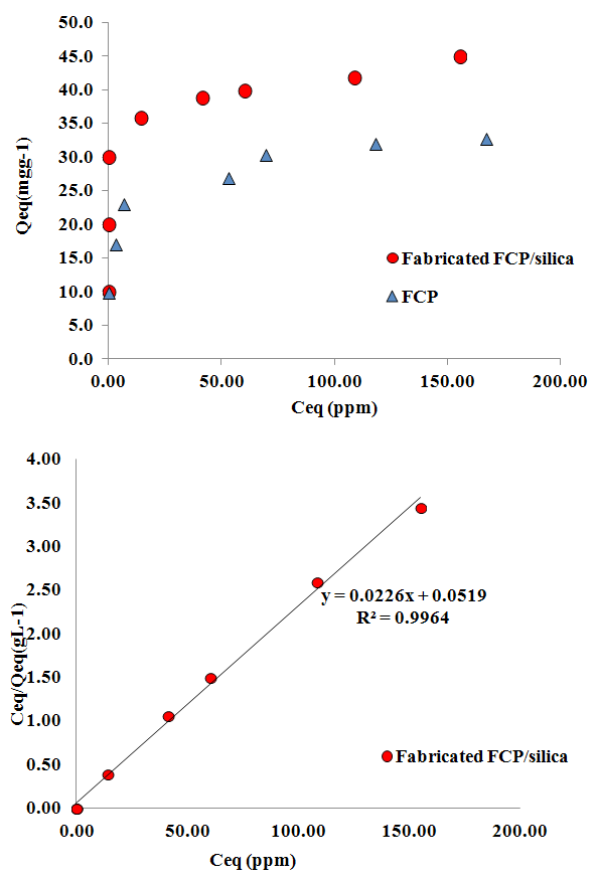


Fig. 9. Adsorption isotherms of Pb(II) on fabricated FCP/silica gel at pH = 5.5 and 25°C.

adsorption of Pb(II) on silica gel at pH 5.15 [46]. Kushwaha et al. functionalized silica gel with 2-thiophenecarbonyl, 2-furoyl and L-proline to increase the q_m value from 15.62 mg/g for silica gel to reach 22.2 mg/g for silica gel functionalized with L-proline [47].

It is worth to mention that both FCP and fabricated FCP-silica were found to be very effective in removal of

Table 4
Calculated values of Langmuir parameters for the adsorption of Pb(II), Cd(II) and $\text{Cr}_2\text{O}_7^{2-}$ onto FCP and JCP at 25°C

FCP					
Langmuir isotherm					
Metal	q_m (mg/g)	q_m (mmol/g)	K_L (L/mg)	K_L (L/mmol)	R^2
Pb(II)	33.00	0.159	0.24	49.73	0.9962
Cd(II)	24.69	0.219	0.14	15.74	0.9950
Cr(VI)	56.50 (117.35)*	1.087	0.04	2.080	0.9994
JCP					
Langmuir isotherm					
Metal	q_m (mg/g)	q_m (mmol/g)	K_L (L/mg)	K_L (L/mmol)	R^2
Pb(II)	54.94	0.265	0.09	18.648	0.9924
Cd(II)	20.08	0.179	0.04	4.496	0.9967
Cr(VI)	54.05 (112.26)*	1.040	0.02	1.040	0.9938

Pb(II) from relatively low concentrations of Pb(II) (less than 30 ppm) with 100% uptake in the case of fabricated FCP-silica (Figs. 8 and 9). This efficiency is due to the remarkably high K_L value obtained in the case of fabricated FCP/silica ($K_L = 0.44$ L/mg) and FCP ($K_L = 0.24$ L/mg). It is worth mentioning that K_L values reported for adsorption of Pb(II) on silica gel were also large 0.129 [46] and 0.2375 [47]. This may indicate that silica gel play a role in increasing the K_L value of fabricated FCP/silica.

3.2.4. Kinetics of adsorption of metal ions on FCP and JCP

The rate of adsorption of Pb(II) and Cd(II) at pH 5.5 and $\text{Cr}_2\text{O}_7^{2-}$ at pH 2.0 onto FCP and JCP was investigated by batch equilibration technique as a function of contact time ranging from 5 min (300 s) to 32 h. The initial adsorption rates of Pb(II), Cd(II) and $\text{Cr}_2\text{O}_7^{2-}$ were calculated directly by subtracting the concentration of metal ion at a contact time of 300 s from the initial concentration and dividing by 300 s. The values obtained were -4.9×10^{-7} , -6.9×10^{-7} and -1.378×10^{-6} mol/L.s, respectively, in the case of FCP and -5.0×10^{-7} , -5.9×10^{-7} and -2.8×10^{-6} mol/L.s, respectively in the case of JCP. The results revealed that the order of the initial adsorption rate was: $\text{Cr}_2\text{O}_7^{2-} \gg \text{Cd(II)} > \text{Pb(II)}$ and the values of FCP were close to those on JCP. The high initial adsorption rates of $\text{Cr}_2\text{O}_7^{2-}$ compared with Pb(II) and Cd(II) may be due to an electrostatic mechanism of interaction, while heavy metal cations are chemically bonded.

Many kinetics models are available in the literature for fitting adsorption uptake as a function of time. They include pseudo first order, pseudo second order and intra-particle diffusion models. Pseudo-second-order was found

to have the best fitting for the data of the present work. This model is based on the assumption that the rate limiting step is chemisorption [48]. The pseudo-second-order reaction kinetic model can be represented as [49]:

$$\frac{dq_t}{dt} = k_2(q_e - q_t)^2 \quad (10)$$

where k_2 is the second order reaction constant ($\text{g mg}^{-1} \text{s}^{-1}$), q_e and q_t are the amount of metal ions adsorbed per unit mass of adsorbent at equilibrium and time t , respectively. Integrating Eq. (10) for the boundary conditions $t = 0$ to $t = t$ and $q_t = 0$ to $q_t = q_e$ gives:

$$\frac{t}{q_t} = \frac{1}{k_2 q_e^2} + \frac{t}{q_e} \quad (11)$$

From the plots of pseudo second order model (t versus t/q_t) in Fig. 10, the equilibrium amount of adsorbed metal ion q_e and the rate constants k_2 for adsorption processes could be calculated. The results (Table 5) indicated that the rate constants (k_2) of adsorption of metal ions on JCP are much higher than FCP. This is due to the fact that JCP contains more acidic sites (carboxylic and phenolic) than FCP as indicated by elemental analysis and pH titration studies (Sections 3.1.2 and 3.1.3).

The equilibrium amounts of adsorption q_e obtained from pseudo second order model do not offer an accurate measure of adsorption capacity of metal ions because it depends on 100 ppm initial concentration of metal ion which does not necessarily satisfy the conditions of saturation. So q_e will not be discussed here because the q_m obtained from Langmuir adsorption model (Section 3.2.3) was considered for comparison between metal ions, FCP and JCP.

Table 5 shows that the rate constant (k_2) of adsorption of dichromate anion ($\text{Cr}_2\text{O}_7^{2-}$) is lower than that of metal cations Pb(II) and Cd(II). This may be due to that Pb(II) and Cd(II) have adsorption mechanism differ from that of $\text{Cr}_2\text{O}_7^{2-}$. In the case of FCP, Cd(II) was found to have higher adsorption rate constant (1.09×10^{-4}) than Pb(II) (4.96×10^{-6}) because the former has smaller ionic size (0.95 Å) than the latter (1.2 Å).

Shaker et al. reported k_2 value of $7.33 \times 10^{-5} \text{ g mg}^{-1} \text{ s}^{-1}$ for adsorption of Cr(VI) on HA at pH = 5.5 [38]. This

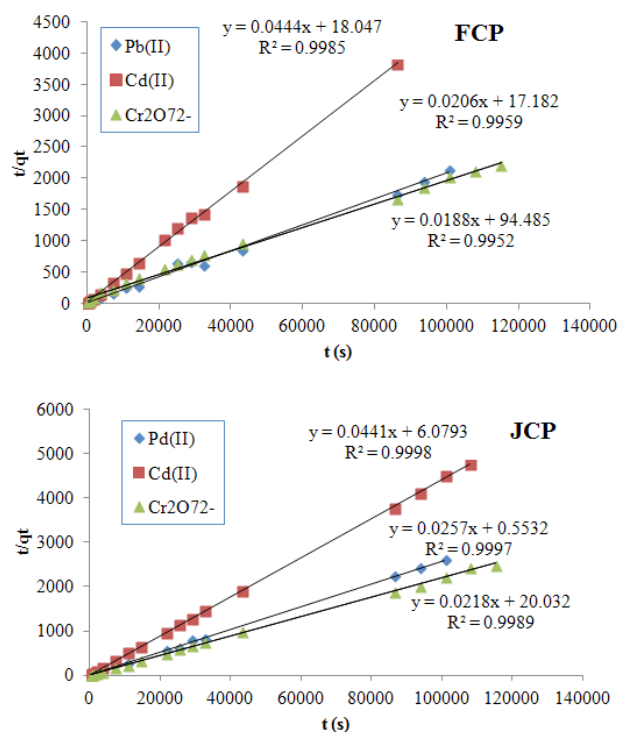


Fig. 10. Pseudo second order plots for the adsorption of Pb(II), Cd(II), and $\text{Cr}_2\text{O}_7^{2-}$ ion on FCP and JCP.

Table 5
Pseudo-second-order parameters for adsorption of Pb(II), Cd(II), Fe(III), and $\text{Cr}_2\text{O}_7^{2-}$ on FCP and JCP

CP	$q_{e, \text{exp.}}$ (mg/g)	$q_{e, \text{calc.}}$ (mg/g)	k_2 ($\text{g mg}^{-1} \text{s}^{-1}$)	R^2
Pb(II)				
FCP	63.32	62.11	4.96×10^{-6}	0.9922
JCP	38.9	38.91	1.19×10^{-3}	0.9997
Cd(II)				
FCP	22.90	22.52	1.09×10^{-4}	0.9985
JCP	22.80	22.68	3.20×10^{-4}	0.9998
Cr(VI)				
FCP	52.50	53.19	3.74×10^{-6}	0.9952
JCP	46.40	45.87	2.37×10^{-5}	0.9989

rate constant was slightly higher than the rate constants obtained in the present work for adsorption of Cr(VI) on FCP and JCP (3.74×10^{-6} and 2.37×10^{-5} g/mg.s) due to the compact nature of the coupling products (as shown in the SEM, section 3.1.6.) compared with free HA.

The k_2 reported for adsorption of Pb(II) on free chitosan was 2.11×10^{-4} g/mg.s. This value was reduced to 2.17×10^{-5} g mg⁻¹ s⁻¹ in the case of chitosan cross-linked with tripolyphosphate [14]. The values of cross-linked chitosan were comparable to those obtained in the case of JCP in the present work (2.37×10^{-5} g/mg.s). Thus, the coupling reaction between chitosan and JHA is like crosslinking of chitosan with tripolyphosphate causing reduction in k_2 (as well as reduction in q_m , Section 3.2.3) relative to free chitosan. Similar values of rate constant k_2 were obtained for adsorption of Pb(II) on chitosan cross-linked using glutaraldehyde (7.32×10^{-5} g mg⁻¹ s⁻¹) [13], for adsorption of Cd(II) chitosan nanoparticles prepared by emulsion-crosslinking method (2.02×10^{-5} g/mg.s) [34] and for adsorption of Pb(II) on chitosan crosslinked with EDTA (4.40×10^{-5} g/mg.s) [25].

3.2.5. Thermodynamics of adsorption

Thermodynamic parameters, including ΔG° , ΔH° and ΔS° were calculated using Eq. (12):

$$\ln K_d = \Delta S^\circ / R - \Delta H^\circ / RT \tag{12}$$

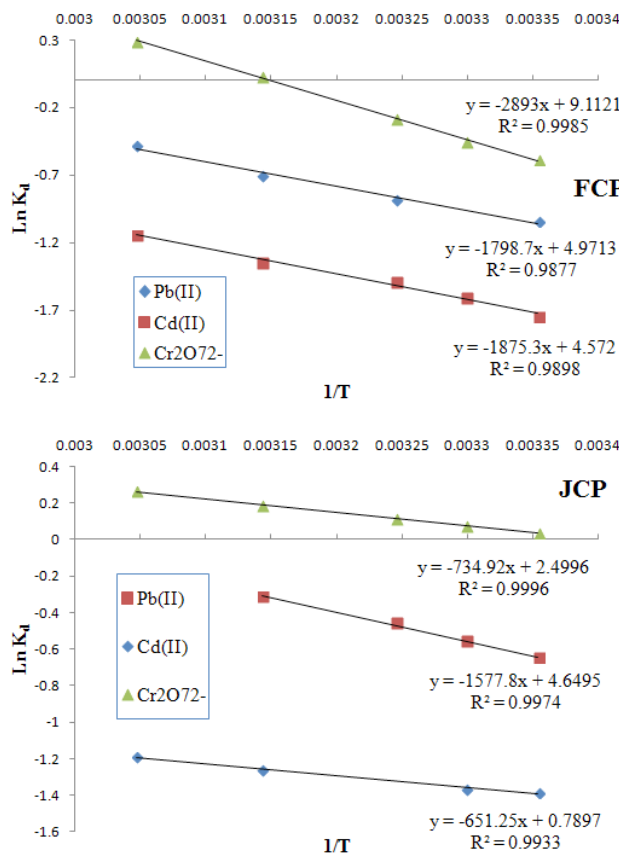


Fig. 11. Plot of $\ln K_d$ of Pb(II), Cd(II), Cr₂O₇²⁻ as a function of temperature for FCP and JCP.

where K_d is the equilibrium constant or distribution coefficient which is defined as the amount of metal ion adsorbed divided by the amount in solution [50]:

$$K_d = \frac{q_e}{C_e} \tag{13}$$

R is the gas constant and T is the temperature in Kelvin. The plot of $\ln K_d$ against $1/T$ for each metal ion (Fig. 11) gives a linear relationship, where the values of enthalpy (ΔH°) and entropy (ΔS°) were obtained from the slope and intercept, respectively. ΔG° was calculated at 25°C using Eq. (14) and the results are given in Table 6.

$$\Delta G^\circ = \Delta H^\circ - T \Delta S^\circ \tag{14}$$

The results indicated positive values for ΔH° and ΔS° . Thus, the adsorption of metal ions on the coupling products is an endothermic process associated with an increase in entropy. One possible explanation of the endothermicity of heats of adsorption is that the metal ions are well solvated.

Tables 6
Thermodynamic parameters for adsorption of metal ions on FCP and JCP

CP	ΔG° (kJ/mol)	ΔH° kJ/mol	ΔS° J/K-mol
Pb(II)			
FCP	2.48	15.84	44.40
JCP	1.60	13.12	38.66
Cd(II)			
FCP	4.32	15.59	38.01
JCP	3.44	54.14	6.57
Cr(VI)			
FCP	1.47	24.05	75.76
JCP	-0.0893	6.11	20.78

Table 7
% Desorption of metal ions from FCP and JCP

Leaching solution	FCP		
	Pb(II)	Cd(II)	Cr ₂ O ₇ ²⁻
HCl	95.93	90.61	77.33
HNO ₃	90.82	90.82	77.84
H ₂ SO ₄	76.81	76.81	75.81
NaCl	88.03	88.03	67.94
NaNO ₃	95.68	95.68	67.79
	JCP		
HCl	68.22	84.48	66.81
HNO ₃	68.88	84.30	63.75
H ₂ SO ₄	66.26	86.37	64.71
NaCl	67.36	82.20	60.83
NaNO ₃	64.25	82.54	61.49

In order for the metal ions to be adsorbed, they have to lose part of their hydration shell. This dehydration process requires energy and increases the entropy. This energy of dehydration supersedes the exothermicity of the ions getting attached to the surface.

3.2.6. Desorption experiments

The aim of this part of study is to test the possibility of regeneration of FCP and JCP loaded with Pb(II), Cd(II) and $\text{Cr}_2\text{O}_7^{2-}$. Five desorbing agents, 0.2 M of HCl, M HNO_3 , M H_2SO_4 , M NaCl and M NaNO_3 (100 mL each) were used for desorbing metal ions loaded onto FCP and JCP at 25°C and 24 h of shaking time. The results are given in Table 7. It is clear that all these salts and acidic solutions are effective for desorbing metal ions from the loaded coupling products up to 96% efficiency. Thus, the coupling products can be regenerated easily.

4. Conclusions

Humic acid and chitosan could be immobilized effectively by coupling with each other. Both contain plenty of active functional sites for adsorption of metal ions that remains after coupling reaction. Furthermore, the coupling reaction can be carried out in the presence of large surface area particles like silica gel in order to spread the coupling product to achieve high adsorption efficiency.

Cross-linking of chitosan with humic acid is better than the reported cross-linking with glutaraldehyde or triphosphosphate because humic acid provides more active sites for adsorption. Furthermore, the coupling products prepared in the present article are effective in removal of metal cations Pb(II) and Cd(II) and anions ($\text{Cr}_2\text{O}_7^{2-}$).

Chitosan interacts with humic acid through formation of electrostatic adduct between the $\sim\sim\text{NH}_3^+$ of chitosan with the carboxylate ($-\text{OOC}\sim\sim$) of humic acid. Pb(II), Cd(II) and $\text{Cr}_2\text{O}_7^{2-}$ could interrupt this bridge by chelation of metal cation with the carboxylate and the electrostatic interaction of dichromate anion with the ammonium group.

Symbols and abbreviations

C_e	— Equilibrium concentration of metal ion in solution (mg/L)
FCP	— Coupling product of Fluka humic with chitosan
FHA	— Fluka humic acid
HA	— Humic acid
JCP	— Coupling product of Ajloun-Jordan humic with chitosan
JHA	— Ajloun-Jordan humic acid
k_2	— The second order reaction constant (g/mg.min)
K_L	— Langmuir affinity constant (L/mg)
q_e	— the equilibrium amount of metal ion adsorbed per unit mass of adsorbent (mg/g)
q_m	— Langmuir monolayer adsorption capacity (mg/g)
q_t	— The amount of metal ions adsorbed (mg/g) at contact time t

References

- [1] G. Ziemacki, G. Viviano, F. Merli, Heavy metals: sources and environmental presence, *Ann. Ist. Super. Sanità*, 25 (1989) 531–536.
- [2] J.O. Duruibe, M.O.C. Ogwuegbu, J.N. Ekwurugwu, Heavy metal pollution and human biotoxic effects, *Int. J. Phys. Sci.*, 2 (2007) 112–118.
- [3] M. Wana, C. Kan, B.D. Rogel, L.P. Dalida, Adsorption of copper (II) and lead (II) ions from aqueous solution on chitosan-coated sand, *Carbohydr. Polym.*, 80 (2010) 891–899.
- [4] S. Malar, S. Vikram, P. Favas, V. Perumal, Lead heavy metal toxicity induced changes on growth and antioxidative enzymes level in water hyacinths [*Eichhornia crassipes* (Mart.)], *Botanical Studies*, 54 (2014) 1–11.
- [5] D. Tilaki, R. Ali, Study on removal of cadmium from water environment by adsorption on GAC, BAC and biofilter, *Diffuse Pollution Conference*, Dublin, 8B Ecology, (2003) 35–39.
- [6] A.L. Mendoza, J.L. Reyes, E. Melendez, D. Martín, M.C. Namorado, E. Sanchez, L.M. Del, Alpha-tocopherol protects against the renal damage caused by potassium dichromate, *Toxicology*, 218 (2006) 237–246.
- [7] K.A. Patlolla, C. Barnes, D. Hackett, P.B. Tchollnwou, Potassium dichromate induced cytotoxicity, genotoxicity and oxidative stress in human liver carcinoma (HepG2) cells, *Int. J. Environ. Res.*, 6 (2009) 643–653.
- [8] D.P. Vihol, J. Patel, R.D. Varia, J.M. Pater, D.G. Ghodasara, B.P. Joshi, K.S. Prajapati, Effect of sodium dichromate on haemato-biochemical parameters in wistar rats, *J. Pharmacology*, 7 (2012) 58–63.
- [9] X. Zhang, R. Bai, Mechanisms and kinetics of humic acid adsorption onto chitosan-coated granules, *J. Colloid Interf. Sci.*, 264 (2003) 30–38.
- [10] S. Malkondu, A. Kocak M. Yilmaz, Immobilization of two azacrown ethers on chitosan: evaluation of selective extraction ability toward Cu(II) and Ni(II), *J. Macromol. Sci.—Part A: Pure Appl. Chem.*, 46 (2009) 745–750.
- [11] W.S. Wan Ngah, A. Musa, Adsorption of humic acid onto chitin and chitosan, *J. Appl. Polym. Sci.*, 69 (1998) 2305–2310.
- [12] J. Kumirska, M. X. Weinhold, J. Thoming, P. Stepnowski, Bio-medical activity of chitin/chitosan based materials—influence of physicochemical properties apart from molecular weight and degree of N-Acetylation, *Polymers*, 3 (2011) 1875–1901.
- [13] Y. Lu, J. He, G. Luo, An improved synthesis of chitosan bead for Pb(II) adsorption, *Chem. Eng. J.*, 226 (2013) 271–278.
- [14] J.B. Dima, C. Sequeiros, N.E. Zaritzky, Hexavalent chromium removal in contaminated water using reticulated chitosan micro/nanoparticles from seafood processing wastes, *Chemosphere*, 141 (2015) 100–111.
- [15] E. Ghabbour, G. Davies, Humic substances (structures, models and function). Royal Society of Chemistry, UK, pp. 19–30.
- [16] B. El-Eswed, F. Khalili, Adsorption of Cu(II) and Ni(II) on solid humic acid from the Azraq area, Jordan, *J. Colloid Interf. Sci.*, 299 (2006) 497–503.
- [17] H. Baker, F. Khalili, Analysis of the removal of lead(II) from aqueous solutions by adsorption onto insolubilized humic acid: temperature and pH dependence. *Anal. Chim. Acta*, 516 (2004) 179–186.
- [18] J. Zhao, G. Binjiang, Coating Fe_3O_4 Magnetic nanoparticles with humic acid for high efficient removal of heavy metals in water, *Environ. Sci. Technol.*, 42 (2008) 6949–6954.
- [19] W.L. Yan, R. Bai, Adsorption of lead and humic acid on chitosan hydrogel beads, *Water Res.*, 39 (2004) 688–698.
- [20] W.S. Wan Ngah, M.A. Hanafiah, S.S. Yong, Adsorption of humic acid from aqueous solutions on crosslinked chitosan-epichlorohydrin beads: Kinetics and isotherm studies, *Colloid Surface B: Biointerfaces*, 65 (2008) 18–24.
- [21] S.J. Santosa, D. Siswanta, A. Kumiawan, W.H. Rahmanto, Hybrid of chitin and humic acid as high performance sorbent for Ni(II), *Surf. Sci.*, 601 (2007) 5155–5161.
- [22] S.J. Santosa, D. Siswanta, S. Sudiono, M. Sehol, Synthesis and utilization of chitin-humic acid hybrid as sorbent for Cr(III), *Surf. Sci.*, 601 (2007) 5148–5154.

- [23] E. Repo, J.K. Warchol, T.A. Kurniawan, M.E.T. Sillanpää, Adsorption of Co(II) and Ni(II) by EDTA- and/or DTPA-modified chitosan: kinetic and equilibrium modeling, *Chem. Eng. J.*, 161 (2010) 73–82.
- [24] F. Zhao, E. Repo, D. Yin, M.E.T. Sillanpää, Adsorption of Cd(II) and Pb(II) by a novel EGTA-modified chitosan material: Kinetics and isotherms, *J. Colloid Interface Sci.*, 409 (2013) 174–182.
- [25] F. Zhao, E. Repo, M. Sillanpää, Y. Meng, D. Yin, W.Z. Tang, Green synthesis of magnetic EDTA- and/or DTPA-cross-linked chitosan adsorbents for highly efficient removal of metals, *Ind. Eng. Chem. Res.*, 54 (2015) 1271–1281.
- [26] A. Rodrigues, A. Brito, P. Janknecht, M. F. Proenc, R. Nogueira, Quantification of humic acids in surface water: effects of divalent cations, pH, and filtration *J. Environ. Monit.*, 11 (2009) 377–382.
- [27] Y. Wu, M. Hussain, R. Fassihi, Development of a simple method for determination of glucosamine release from modified release matrix tablets, *J. Pharmaceut. Biomed.*, 38 (2005) 263–269.
- [28] M. Schnitzerin, M. Schnitzer, S. U. Khan, (eds.), *Soil Organic Matter*, Elsevier Scientific Publishing Company (1978) pp. 1–64.
- [29] G. R. Choppin, L. Kullberg, Proton thermodynamics of humic acid. *J. Inorg. Nucl. Chem.*, (40) (1978) 651–654.
- [30] S. Samal, R.R. Das, S. Acharya, P. Mohapatra, R.K.A. Dey, Comparative study on metal ion uptake behavior of chelating resins derived from the formaldehyde–condensed phenolic Schiff bases of 4,4′-diaminodiphenylsulfone and hydroxybenzaldehydes. *Polym. Plast. Technol. Eng.*, 41(2) (2002) 229–246.
- [31] R. von Wandruszka, Humic acids: their detergent qualities and potential uses in pollution remediation, *Geochem. Trans.*, 1 (2000) 10–15.
- [32] A. Barth, Infrared spectroscopy of proteins, *Biochim. Biophys. Acta*, 1767 (2007) 1073–1101.
- [33] J. Coates, Interpretation of Infrared Spectra, A Practical Approach, in R.A. Meyers (Ed.), *Encyclopedia of Analytical Chemistry*, John Wiley & Sons Ltd, (2000) pp. 10815–10837.
- [34] M.A. Shaker, Thermodynamics and kinetics of bivalent cadmium biosorption onto nanoparticles of chitosan-based biopolymers, *J. Taiwan Inst. Chem. Eng.*, 47 (2015) 79–90.
- [35] M.T. Rosado, M. Leonor, T.S. Durat, R. Fausto, Vibrational spectra of acid and alkaline glycine salts, *Vibr. Spectros.*, 16 (1998) 35–54.
- [36] C. Milne, D. Kinniburgh, W. van Riemsdijk, E. Tipping, “Generic NICA-Donnan model parameters for metal-ion binding by humic Substances, *Environ. Sci. Technol.*, 37 (2003) 958–971.
- [37] Q.Z. Wang, X.G. Chen, N. Liu, S.X. Wang, C.S. Liu, X.H. Meng C.G. Liu, Protonation constants of chitosan with different molecular weight and degree of deacetylation, *Carbohydr. Polym.*, 65 (2006) 194–201.
- [38] M.A. Shaker, H.M. Albishri, Dynamics and thermodynamics of toxic metals adsorption onto soil-extracted humic acid, *Chemosphere*, 111 (2014) 587–595.
- [39] D.G. Kinniburgh, W.H. Riemsdijk, L.K. Koopal, M. Borkovec, M.F. Benedetti, M.J. Avena, Ion binding to natural organic matter: competition, heterogeneity, stoichiometry and thermodynamic consistency, *Colloids Surfaces A: Physicochem. Eng. Asp.*, 151 (1999) 147–166.
- [40] M.E. Essington, *Soil and water chemistry: An integrative approach*. 2nd Edition, CRC Press, Boca Raton, FL (2003) p. 179.
- [41] I. Langmuir, the adsorption of gases on plane surfaces of glass, mica and platinum, *J. Am. Chem. Soc.*, 40 (1918) 1362–1403.
- [42] H.R. Tashauoei, H.M. Attar, M.M. Amin, M. Kamali, M. Nikaeen, V. Dastjerdi, Removal of cadmium and humic acid from aqueous solutions using surface modified nanozeolite A. *Int. J. Environ. Sci. Tech.*, 7 (2010) 497–508.
- [43] G. MaKay, J.F. Porter, Equilibrium parameters for the sorption of copper, cadmium and zinc ions onto peat. *J. Chem. Tech. Biotechnol.*, 69 (1997) 309–320.
- [44] J. Hizal, R. Apak, Modeling of copper(II) and lead(II) adsorption on kaolinite–based clay minerals individually and in the presence of humic acid. *J. Colloid. Interface Sci.*, 295 (2006) 1–13.
- [45] A.T. Paulino, M.R. Guilherme, A.V. Reis, E.B. Tambourgi, J. Nozaki, E.C. Muniz, Capacity of adsorption of Pb²⁺ and Ni²⁺ from aqueous solutions by chitosan produced from silkworm chrysalides in different degrees of deacetylation, *J. Hazard. Mater.*, 147 (2007) 139–147.
- [46] H.H. Tran, F.A. Roddick, J.A. O’donnel, Comparison of chromatography and desiccant silica gel for the adsorption of metal ions I. Adsorption and kinetics, *Wat. Res.*, 33 (1999) 2992–3000.
- [47] A.K. Kushwaha, N. Gupta, M.C. Chattopadhyaya, Adsorption behavior of lead onto a new class of functionalized silica gel, *Arab. J. Chem.*, 10 (2017) S81–S89.
- [48] Y.S. Ho, G. McKay, The kinetics of Sorption of divalent metal ions onto Sphagnum moss peat, *Wat. Res.*, 34 (2000) 735–742.
- [49] Y.S. Ho, G. McKay, Sorption of Dye from Aqueous Solution by Peat, *Cheml. Eng. J.*, 70 (1998) 115–124.
- [50] R. Donat, A. Akdogan, E. Erdem, H. Ceti, Thermodynamics of Pb²⁺ and Ni²⁺ Adsorption onto Natural Bentonite from Aqueous Solutions. *J. Colloid Interf. Sci.*, 286 (2005) 43–52.
- [51] M. Giovanela, E. Parlanti, E.J. Soriano-Sierra, M.S. Soldi, M. M. D. Sierra, Elemental compositions, FT-IR spectra and thermal behavior of sedimentary fulvic and humic acids from aquatic and terrestrial environments, *Geochem. J.*, 38 (2004) 255–264.
- [52] M. Tatzber, M. Stemmer, H. Spiegel, C. Katzlberger, G. Haberhauer, A. Mentler, H.M. Gerzabek, FTIR-spectroscopic characterization of humic acids and humin fractions obtained by advanced NaOH, Na₄P₂O₇ and Na₂CO₃ extraction procedures, *J. Plant Nutr. Soil Sci.*, 170 (2007) 522–529.